

# Study of the mixing mechanism of two miscible liquids via visualization and microPIV methodology

Darina Liederhausová<sup>1\*</sup>, Michal Kotek<sup>1</sup>, and Václav Kopecký<sup>1</sup>

<sup>1</sup>Laboratory of physical measurement, Institute for Nanomaterials, Advanced Technology and Innovation, Bendlova 1409/7, Liberec, Czech Republic

**Abstract.** Reducing the channel dimensions within microfluidic systems enhances mass transfer efficiency and enables precise regulation of concentration gradients. A fundamental function of microfluidic devices is the mixing of miscible liquids. One proposed mechanism for liquid mixing in such systems is diffusion, which is predicated on the assumption that, given the low Reynolds numbers and laminar flow conditions typical of microfluidic environments, turbulence does not facilitate mixing. Nonetheless, the mixing efficiency observed is often significant and can be further augmented through the implementation of optimized geometric configurations. The primary methodology employed to assess liquid mixing efficacy involves visualization techniques, such as the use of dyed solutions. However, the visualized outcomes do not directly correlate with theoretical calculations of mixing time based on diffusion processes. This study focuses on the confluence of liquids within a Y-branch microchannel. Utilizing visualization methodologies and the micro-Particle Image Velocimetry (micro-PIV) technique, we aim to elucidate the parameters that influence and optimize effective mixing within this geometric configuration.

## 1 INTRODUCTION

Mixing in passive microchannels presents a fundamental challenge in microfluidic systems, primarily due to the dominance of laminar flow at low Reynolds numbers ( $Re \ll 1$ ). Under such flow conditions, turbulence is absent, and molecular diffusion becomes the primary mechanism for mixing. However, diffusion alone is typically insufficient for rapid homogenization, particularly when dealing with macromolecules or larger channel dimensions. Consequently, a variety of passive micromixer designs have been developed to enhance mixing efficiency by exploiting channel geometry and flow manipulation, without the need for external energy input.

The simplest form of mixing in microchannels is diffusion-based mixing, which relies solely on molecular diffusion across the interface of two laminar fluid streams. This process is governed by the molecular diffusion coefficient and the characteristic diffusion length, such that the diffusion time  $t_D = L^2/D$ , where  $L$  is the characteristic length scale (m) and  $D$  is the diffusion coefficient ( $m^2/s$ ). Although diffusion-based mixing is conceptually straightforward and easy to implement in simple T-junction or Y-junction microchannels, it is often too slow for practical applications involving large molecules or limited residence times.

To improve mixing under laminar conditions, various strategies induce chaotic advection, which involves the generation of complex, time-independent flow patterns that stretch and fold fluid elements. This mechanism increases the interfacial area between different fluid streams, thereby accelerating diffusion. Notable examples include the staggered herringbone mixer (SHM), which incorporates asymmetric grooves on the channel floor to create transverse vortices, and

serpentine or wavy channels, where curvature induces secondary flows known as Dean vortices. Three-dimensional channel geometries that direct fluid motion vertically or laterally can also promote chaotic advection by repeatedly reorienting the flow.

Another important mechanism is the split-and-recombine (SAR) approach, in which the flow is divided into multiple substreams that are subsequently recombined downstream. Each split-and-recombine cycle increases the total interfacial area and reduces the diffusion path length, resulting in progressively enhanced mixing. This strategy is commonly implemented in three-dimensional micromixers or in lamination-type mixers, where multiple fluid layers are stacked and merged repeatedly.

Dean flow-induced mixing represents a related approach that leverages secondary flows arising from centrifugal forces in curved channels. When a fluid moves through a curved path, the imbalance between centrifugal and viscous forces generates counter-rotating vortices, known as Dean vortices, that drive transverse mixing across the channel cross-section. The intensity of this effect is characterized by the Dean number, defined as  $De = Re\sqrt{D_h/(2R)}$ , where  $R$  is the radius of curvature (m) and  $D_h$  is the hydraulic diameter (m). Even at modest Reynolds numbers (typically in the range of 10–100), Dean flows can significantly enhance mixing efficiency.

Further enhancement can be achieved through surface patterning and texturing, in which microstructures such as ridges, grooves, or pillars are introduced along the channel walls. These surface features locally modify the flow field, generating transverse velocity components that disrupt laminar streamlines and promote interfacial mixing. The design and arrangement of these features can be optimized for specific flow conditions and fluid properties.

\* Corresponding author: [darina.jasikova@tul.cz](mailto:darina.jasikova@tul.cz)

Finally, hydrodynamic focusing is a common strategy in which a central fluid stream is compressed by adjacent sheath flows, reducing its cross-sectional area. This confinement decreases the diffusion path length and accelerates the mixing process.

A typical initial geometry, where two liquids meet at different angles, is Y-junction. Analysis of flow in this area is extremely important for understanding the processes that prevail over the principle of natural diffusion. Thanks to the micro-PIV method, it is possible to record and evaluate the characteristics of fluid motion.

## 1.1 Theoretical background

Diffusion is the process of molecules and particle moving from an area of higher concentration to an area of lower concentration due to Brownian motion. The result is an equal, evenly distributed concentration of the substance throughout the volume. It is a time-dependent process and is characterized by the equation:  $d^2 = 2Dt$ , where  $d$  is the distance traveled by particles (m) in time  $t$  (s), and  $D$  is the diffusion coefficient of molecules or particles ( $m^2/s$ ).

However, the central idea of diffusion is common to all areas: a substance or set undergoing diffusion spreads from a point or place where there is a higher concentration of that substance or set. The change in concentration as a function of distance is called the concentration gradient. Diffusion leads to the mixing or transfer of mass without requiring controlled bulk motion. Bulk motion or bulk flow is characteristic of advection. The term convection is used to describe a combination of both transport phenomena.

In continuum mechanics, the Péclet number  $Pe$  (named after J. C. E. Péclet) is defined as the ratio of the advection velocity of a physical quantity by flow to the diffusion velocity of the same quantity driven by the corresponding gradient. In the context of mass or substance transfer,  $Pe$  number is the product of the Reynolds number and the Schmidt number, where the Schmidt number expresses the ratio between the rate of momentum dispersion (kinematic viscosity) and the rate of mass dispersion (mass diffusivity) in each environment.

In general, the Péclet number is defined as:  $Pe = \frac{uw}{D} = Re_L \cdot Sc$ , where  $u$  is the average flow velocity (m/s),  $w$  is the channel width (m), and  $D$  is the diffusion coefficient ( $m^2/s$ ),  $Re$  is the Reynolds number (1), and  $Sc$  is the Schmidt number (1). For  $Pe \gg 1$ , the diffusion time is much longer compared to the transport time, and therefore this phenomenon prevails, which is characteristic of microfluidic flows. Advection is negligible and diffusion dominates. For  $Pe = 1$ , advection and diffusion are in time equilibrium. For  $Pe < 1$  diffusion is negligible and advection dominates.

The proportionality constant between the diffusion flux and the concentration gradient (see diffusion of colloids) is numerically equal to the amount of the diffusing component that passes through a unit area per unit time at a unit concentration gradient ( $m^2/s$ ). Based on hydrodynamic theory, the so-called Einstein equation

was derived for the diffusion coefficient in dilute dispersions of uncharged particles:  $D = \frac{k_B T}{f}$ , where  $k_B$  is Boltzmann's constant  $1.380649 \times 10^{-23}$  J/K,  $T$  is the absolute temperature (K), and  $f$  is the friction coefficient, which is a function of the size of the dispersion particle and the properties of the dispersion environment. The internal friction coefficient is the dynamic viscosity of the liquid.

For spherical particles, the friction coefficient is given by the relationship:  $f = 6\pi\eta r \left( \frac{2\eta + r\beta}{3\eta + r\beta} \right)$ , where  $\eta$  is the dynamic viscosity of the environment (Pa.s),  $r$  is the particle radius (m), and  $\beta$  is the coefficient of sliding friction.

Spherical particles are larger than molecules of water, so the solvent can be considered as a continuum and the friction coefficient  $\beta$  is large, and the friction coefficient can be simplified by expressing it from Stokes' equation:  $f = 6\pi\eta r$ , thus:  $D = \frac{k_B T}{6\pi\eta r}$ .

The above inputs are analytically considered in the Taylor-Aris approach, which is why this type is referred to as Taylor-Aris dispersion [1,2]. We assume that diffusion depends on the transverse gradient of the velocity field, which is controlled by pressure only in the radial direction. Furthermore, the theory includes the average concentration of particles that flow through the mass flow rate across the capillary cross-section. Then, the diffusion efficiency, which depends on the flow velocity, can be expressed as:  $D_{eff} = \frac{R^2 u^2}{48D}$ , where  $R$  is the channel radius (m),  $u$  is the mean flow velocity (m/s), and  $D$  is the standard diffusion coefficient for liquids ( $m^2/s$ ).

The relative ratio between convective and diffusive transport through the microchannel in relation to the Pe number can be expressed as:  $\frac{R^2 u^2}{48D} \gg 7Pe \gg 14$

This condition is considered invalid if another type of electrokinetic strategy prevails in the flow. Controlled diffusion is one of the strategies for inducing mixing of two liquids. In biomicrofluidic systems, mixing is achieved either by passive mechanisms [3,4] or by an external energy field.

A preliminary numerical analysis determined that  $Pe = 31.106$  for a volumetric flow rate of  $0.1 \text{ mL} \cdot \text{h}^{-1}$ , corresponding to an average injection velocity of  $0.00023 \text{ m} \cdot \text{s}^{-1}$ . This value indicates that advection dominates over molecular diffusion under these operating conditions. A high Pe number necessitates the use of strategies that increase the interfacial area while simultaneously reducing the diffusion path length. These objectives can be achieved through passive methods such as serpentine channel geometries or flow divisions or by employing active mixing elements.

The geometric configuration of the channel significantly influences fluid behaviour, particularly at the point where streams merge or encounter a sudden expansion. In such regions, flow redirection and local disturbances can occur even at low flow rates, occasionally leading to the formation of vortices. As the volumetric flow rate increases, the  $Re$  rises, indicating a higher ratio of inertial to viscous forces. When  $Re$  reaches the transitional or turbulent regime, localized

vortical structures and unsteady flow patterns develop. These instabilities disrupt the laminar interface between the streams and consequently enhance mixing efficiency.

When identical flow rates are introduced through two inlet branches of equal cross-section, and one branch contains a known concentration of suspended particles, diffusion proceeds from the saturated to the unsaturated stream. Along the length of the channel, the concentration gradients between the two flows gradually diminish. This process is governed jointly by advection and molecular diffusion. The mixing rate depends on the flow velocity, fluid viscosity, and particle diffusivity.

At low volumetric flow rates, the flow remains laminar, preserving a stable interface and providing sufficient time for diffusion. Conversely, at high flow rates, advection suppresses diffusion, preventing complete concentration equilibration within the given channel length. Thus, effective mixing by diffusion requires slow, stable, and laminar flow conditions.

Experimental verification of diffusion is inherently challenging. The principal limitation arises from the restricted spatial and temporal resolution of optical measurement techniques, which may be insufficient to resolve subtle concentration variations near the interface. Additional complications include the physical characteristics of tracer particles, their interactions with channel walls, and potential side effects that can distort the observed diffusion profile.

## 2 Experimental solution

### 2.1 Channel Geometry

The experiments were conducted using a microfluidic Y-channel with the following dimensions: Inlet branches (a, b):  $1.0 \times 0.140$  mm, Straight section:  $1.4 \times 0.140$  mm, Expansion section:  $2.8 \times 0.140$  mm. This configuration allows for controlled merging of two streams and the observation of the resulting interfacial dynamics.

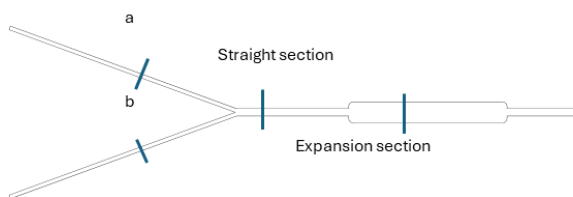


**Fig. 1.** Schema of the microfluidic Y-junction channel with dimensions.

### 2.2 Working Fluids and Physical Properties

The experimental investigation was performed in two sequential phases:

Phase I:

Both inlets (A and B) were supplied with water having a density  $\rho = 997$  kg·m<sup>-3</sup> and dynamic viscosity  $\eta = 0.0010005$  N·s·m<sup>-2</sup> at 20 °C. The flow through inlet A was saturated with Rhodamine B (RhB) particles of 2 μm diameter. The diffusion coefficient of these particles

in water was  $D_p = 7.3 \times 10^{-12}$  m<sup>2</sup>·s<sup>-1</sup>, while the self-diffusion coefficient of water was  $D_w = 2.3 \times 10^{-9}$  m<sup>2</sup>·s<sup>-1</sup>.

Phase II:

Inlets A and B were supplied with water and 99% anhydrous glycerol, respectively, allowing the study of diffusion and mixing under varying viscosities and densities.

### 2.3 Flow Visualization

At the Y-branch junction, where the two streams converge, minor changes in flow direction and curvature induce weak shear gradients and localized convective effects. These effects enhance interfacial contact and can contribute to improved mixing. Flow behaviour in this region was analysed using the micro-Particle Image Velocimetry (micro-PIV) technique, enabling quantitative assessment of velocity fields and local flow structures.

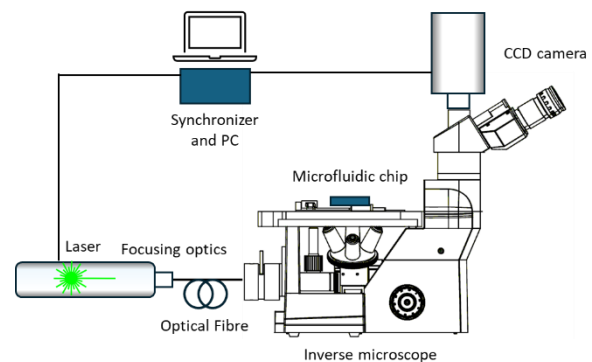


**Fig. 2.** Schema of micro-PIV experimental setup based on inverse microscope, laser, ccd camera and synchronizer.

The micro-PIV system consisted of a NewWave Gemini Nd:YAG pulsed laser. Images were captured using a Neo CMOS camera. The laser and camera system were controlled by a computer and synchronized via an external Timer Box. An inverted Leica microscope was used as the optical component, equipped with a 4× eyepiece magnification and a 5× objective magnification.

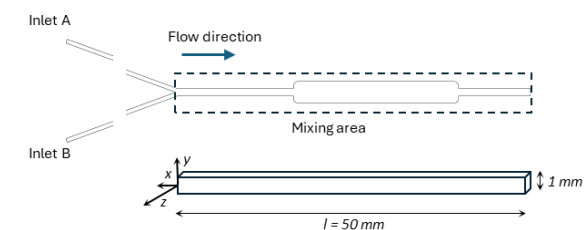


**Fig. 3.** Schema microfluidic chip with marked inlets, mixing area and flow direction.

## 3 Results

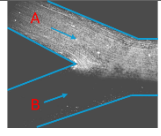
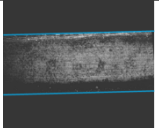
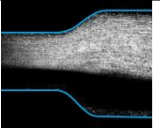
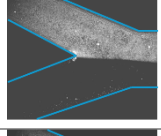
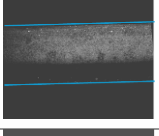
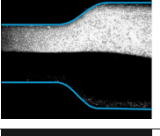
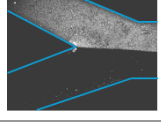
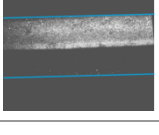
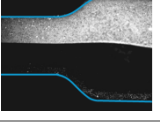
Three liquid flow rates were selected for the measurements: 0.1 mL·h<sup>-1</sup>, 1 mL·h<sup>-1</sup>, and 10 mL·h<sup>-1</sup>, corresponding to average flow velocities of  $1.5 \times 10^{-5}$  m·s<sup>-1</sup>,  $1.5 \times 10^{-4}$  m·s<sup>-1</sup>, and 0.015 m·s<sup>-1</sup>, respectively. These values correspond to Reynolds numbers in the inlet branches of 0.03, 3.6, and 36, indicating that the

flow remained within the laminar regime. When the Reynolds number was calculated for the combined channel, the corresponding values were 0.078, 7.7, and 78.

Initially, 200 images were recorded for visualization analysis to observe changes in particle position over time as a function of flow rate. The image analysis revealed that at a flow rate of  $0.1 \text{ mL}\cdot\text{h}^{-1}$ , the flow underwent an immediate change in direction just downstream of the junction, where the saturated particles spread across the entire channel width. A similar, though less pronounced, trend was observed in both the straight and expanded sections of the channel.

At higher flow rates, namely  $1 \text{ mL}\cdot\text{h}^{-1}$  and  $10 \text{ mL}\cdot\text{h}^{-1}$ , a distinct separation between the two phases the saturated and unsaturated liquids was observed. No mixing occurred under these conditions, and both streams maintained a perfectly parallel co-flow. At the interface between the liquids, a slight stagnation of particles was detected, emphasized by the increased brightness along the separation line.

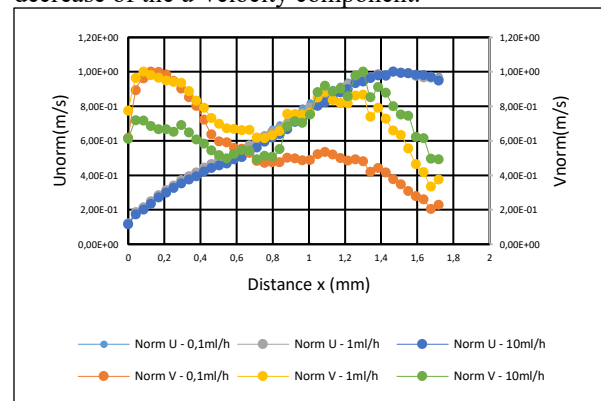
**Table 1.** Result of image analysis summarization to demonstrate particle concentration changes over time for different flow rates of two phases: water – water.

Flow rate	Y – junction	Straight section	Expansion section
0,1 ml/h			
1 ml/h			
10 ml/h			

Another analysis to prove the mechanisms of liquid mixing was to run the x-axis through the centre of the branch and evaluate the velocity vectors and their components in the direction of the x-axis, i.e., the velocity component, and in the direction of the y-axis, i.e., the velocity component. Since the flow rate varied by an order of magnitude from  $0.1 \text{ ml/h}$ ,  $1 \text{ ml/h}$ , and  $10 \text{ ml/h}$ , it was necessary to normalize the increasing velocity so that the velocity profiles were mutually comparable. The normalization of the velocity components  $u$  and  $v$  were always performed to the maximum value.

The evaluation of the data indicates that the normalized  $u$ -velocity remains practically unchanged across different flow rates. The normalized  $v$ -velocity component, corresponding to the direction along the  $y$ -axis, is responsible for the mixing of the two phases. Since the diffusion coefficient of the particles is small, the interpenetration of the phases must be caused by another phenomenon. It can be inferred that this effect

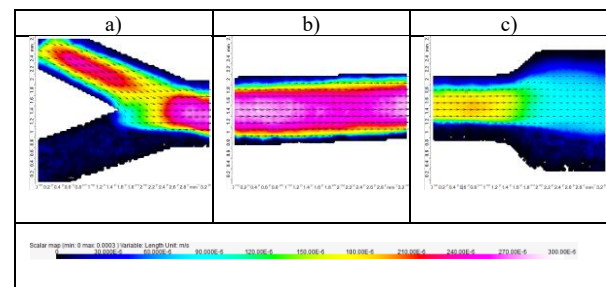
arises from the geometry of the Y-junction, where a sudden channel expansion and the interaction of the two streams at an angle lead to the action of inertial forces between the fluids. The  $v$ -velocity component thus plays a significant role. This component reaches its maximum value immediately after the expansion and gradually decreases downstream. The mixing of fluids with low viscosity and density induces instabilities, which manifest as a secondary increase in this velocity component. The velocity measurement results are consistent with the visual observations. While a simple visual analysis might suggest that the observed behaviour results from diffusion, micro-PIV measurements have revealed a different yet equally important mechanism of mixing and phase interpenetration namely, the increase and subsequent decrease of the  $u$ -velocity component.



**Graph 1.** Evaluation of velocity components  $u$ ,  $v$  along the central axis of the channel. Water-water mixing situation.

At other flow rates, the particles follow the flow determined primarily by advection, while diffusion becomes even less significant. At higher volumetric flow rates, flow instabilities also become more prominent, which are manifested in subsequent sections of the channel as an increase in the  $v$ -velocity component. This phenomenon can be explained by the advection of instabilities downstream by the flow. Further investigation of this effect should focus on a frequency analysis of flow instabilities in this region.

**Table 2.** Vector and scalar map of flow velocity distribution: water – water for flow rates  $Q = 0.1 \text{ ml/h}$  in a symmetrical Y-junction, a) situation in the branch, b) situation in the straight section, c) situation in the expansion section.



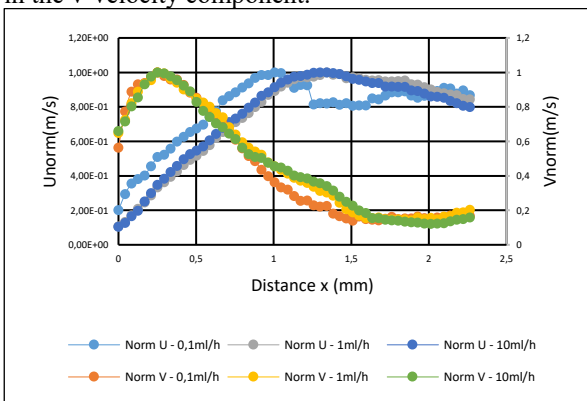
A representative vector and scalar map of the velocity distribution at the confluence of the two phases for a flow rate of  $0.1 \text{ ml/h}$  is presented in Table 3. The figures clearly show changes in flow velocity at the junction, as well as instabilities in the central region of

the microstructure. In the channel expansion zone, a noticeable flow deceleration and change in flow direction can be observed.

**Table 3.** Result of image analysis summary for evidence of particle concentration change over time for different flows of two phases: water – glycerine.

Flow rate	Y – junction	Straight section	Expansion section
0,1 ml/h			
1 ml/h			
10 ml/h			

In the second experiment, the mixing effect was enhanced using easily diffusing liquids specifically glycerol, which is highly soluble in water due to its polarity. Water diffuses into glycerol more readily because of its smaller molecular size. The diffusion coefficient of glycerol into water is approximately  $0.9 \times 10^{-10} \text{ m}^2/\text{s}$ , while the diffusion of water into glycerol representing the relevant case of the mixed medium in this study is around  $1 \times 10^{-10} \text{ m}^2/\text{s}$ . Evidence of diffusion should therefore be supported by a corresponding change in the velocity field, particularly by an increase in the v-velocity component.



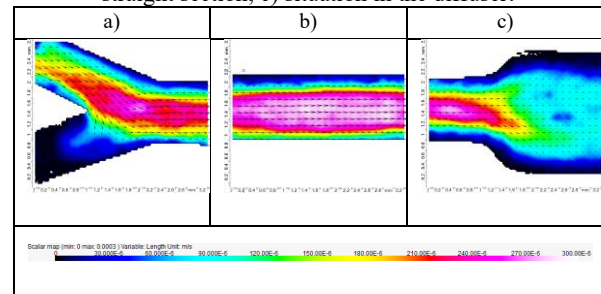
**Graph 2.** Evaluation of velocity components  $u$ ,  $v$  along the central axis of the channel. Water-glycerine mixing situation.

Image analysis clearly shows that at a low flow rate of 0.1 ml/h, a sharp change occurs in the flow direction of the particle-saturated water stream as it enters the glycerol flow. This effect can be attributed to the interaction of interfacial forces, liquid and particle diffusion, and concentration gradients. In the next step, a velocity field analysis was performed, following the same procedure as in the case of the confluence of two

water streams. The  $u$  and  $v$  velocity components, corresponding to the directions along the  $x$ - and  $y$ -axes, respectively, were evaluated and subsequently normalized to their maximum values.

The normalized  $u$  and  $v$  velocity components overlap, indicating that their mutual ratio remains constant across all flow rates. This also implies a significant contribution of diffusion to the  $v$ -velocity component. The directionality of this component can be influenced by the inlet geometry and the angle formed between the inlet branches. This represents an important finding that cannot be determined by any method other than micro-PIV and once again opens possibilities for further investigation. Moreover, this observation provides room for discussion regarding the characteristics of the particles, as in the previous case, and suggests potential pathways for optimizing the velocity field approaches that do not necessarily rely solely on extending the contact length, as is typical in current research directions.

**Table 4.** Vector and scalar map of flow velocity distribution: water – glycerol for flow rates  $Q = 0.1 \text{ ml/h}$  in a symmetrical Y-junction, a) situation in the branch, b) situation in the straight section, c) situation in the diffuser.



The analysis of the velocity fields for the individual flow rates revealed that the interaction of two fully miscible phases occurs immediately upon contact and is facilitated both by the nature of the flow and the properties of the liquids. At this stage, it is necessary to more strongly account for the effects of additional interfacial interactions when designing the experiment and the apparatus. In the downstream regions of the microstructure, the phases are already mixed, and measurements correspond to an aqueous solution with approximately 45% glycerol, exhibiting its behaviour in the straight channel section where flow instabilities are more pronounced.

## 4 Conclusions

With increasing volumetric flow rates of the liquids, the  $v$ -velocity component rises, influencing the mutual interpenetration of the fluids, particularly in the region of the sudden expansion, i.e., at the Y-junction boundary. In this region, a stagnation point of the fluid is observed, which is subsequently accelerated. The flow exhibits stratified 3D behaviour, with successive layers sliding over one another and thus intermixing. Analytical evaluation showed that this velocity is orders of magnitude higher than diffusion, and the Peclet number for a flow rate of 0.1 ml/h ( $v_{\text{inlet}} = 0.00023 \text{ m/s}$ )

was calculated as  $3.1 \times 10^7$ , indicating that mass transport is dominated by advection. At higher volumetric flow rates of both liquids, advection is further enhanced, and in the case of co-flowing streams, separation and stratification of the flows occur. Under these conditions, diffusion is negligible.

In contrast, for freely miscible liquids such as water–glycerol, interfacial interactions become significant, and mixing occurs immediately upon contact at low flow rates. At higher flow rates, stratified flow is again observed. Micro-PIV data analysis revealed the dominant role of the *v*-velocity component. Since the flow remains in the laminar regime, contributions from vortical structures to mixing cannot be expected.

At low flow rates, visualization demonstrated the penetration of particles between the phases. This penetration is facilitated by changes in flow direction and the increasing *v*-velocity component immediately after the confluence. If penetration did not occur directly at the branching, the prevailing advective mass transfer prevented particles from entering the second phase.

Experimentally, the influence of very low volumetric flow rates on fluid mixing was confirmed. Although advective flow velocities are orders of magnitude greater than diffusion, velocity components shaped by the microstructure geometry significantly promote mixing. This process supports the formation of large vortical structures with slow flow characteristics, in contrast to turbulent structures. It is crucial to prevent co-flow and stratified flow to enhance effective mixing.

## References

1. Qian J.Y., Li X.J., Wu Z., Jin Z.J., Sunden B. A comprehensive review on liquid–liquid two-phase flow in microchannel: flow pattern and mass transfer. *Microfluidics and Nanofluidics*. 23 (2019) pp. 116.
2. Zhao Y., Chen G., Yuan Q. Liquid–liquid two-phase mass transfer in the T-junction micro-channels. *American Institute of Chemical Engineers Journals*. 53 (2007) pp. 3042–3053.
3. Li G., Pu X., Shang M., Zha L., Su Y. Intensification of liquid–liquid two-phase mass transfer in a capillary microreactor system. *American Institute of Chemical Engineers Journals*. 65 (2019) pp. 334–346.
4. Narasimha R., Sreenivasan K.R. Relaminarization of Fluid Flow. *Advances App Mech*. 19 (1979) pp. 221–309.